

**On the inward drift of runaway electrons during the plateau phase of runaway current**Di Hu<sup>1, a)</sup> and Hong Qin<sup>2,3</sup><sup>1)</sup>*School of Physics, Peking University, Beijing 100871, China.*<sup>2)</sup>*Princeton Plasma Physics Laboratory, Princeton University, Princeton, New Jersey, 08540, USA*<sup>3)</sup>*School of Nuclear Science and Technology and Department of Modern Physics, University of Science and Technology of China, Hefei, 230026, China.*

(Dated: 10 May 2022)

The well observed inward drift of current carrying runaway electrons during runaway plateau phase after disruption is studied by considering the phase space dynamic of runaways in a large aspect ratio toroidal system. We consider the case where the toroidal field is unperturbed and the toroidal symmetry of the system is preserved. The balance between the change in canonical angular momentum and the input of mechanical angular momentum in such system requires runaways to drift horizontally in configuration space for any given change in momentum space. The dynamic of this drift can be obtained by integrating the modified Euler-Lagrange equation over one bounce time. It is then found that runaway electrons will always drift inward as long as they are decelerating. This drift motion is essentially non-linear, since the current is carried by runaways themselves, and any runaway drift relative to the magnetic axis will cause further displacement of the axis itself. A simplified analytical model is constructed to describe such inward drift both in ideal wall case and no wall case, and the runaway current center displacement as a function of parallel momentum variation is obtained. The time scale of such displacement is estimated by considering effective radiation drag, which shows reasonable agreement with observed displacement time scale. This indicates that the phase space dynamic studied here plays a major role in the horizontal displacement of runaway electrons during plateau phase.

PACS numbers: 45.20.Jj &amp; 52.20.Dq

---

<sup>a)</sup>While visiting at PPPL, Princeton, New Jersey; Electronic mail: hudi\_2@pku.edu.cn

## I. INTRODUCTION

Large quantity of relativistic runaway electrons is one of the most feared by-product of tokamak disruption, especially for large devices with higher total plasma current and higher poloidal magnetic flux<sup>1</sup>. Those highly relativistic electrons are the direct result of high toroidal inductive field during disruption, which in turn is the consequence of drastically arising bulk plasma resistivity as the thermal energy is mostly lost after thermal quench<sup>2,3</sup>. If left unchecked, runaway electrons can multiply exponentially by Coulomb-collision avalanche<sup>1</sup>, and up to 70% of initial plasma current can be converted into relativistic runaway current, forming the so called “runaway current plateau”<sup>4</sup>. Furthermore, the high energy electrons will keep being accelerated until effective radiation drag from synchrotron radiation and bremsstrahlung radiation finally balance the toroidal inductive field<sup>5-7</sup>. This will result in a highly anisotropic relativistic electron beam with energy on the order of tens of MeVs<sup>8</sup>, as well as a “bump on the tail” kind of distribution function in the momentum-space<sup>9-11</sup>.

The evolution of runaway electrons in momentum-space has been under substantial investigation during past decades<sup>5-7,12-14</sup>. However, the corresponding evolution in configuration space has not received due attention. During the aforementioned runaway current plateau, it is widely observed that there is a gradual inward drift of runaway current<sup>15-17</sup>. This inward drift will ultimately result in the intersection between runaway electrons and the wall, causing tremendous damage to the first wall due to its localized way of energy deposition<sup>18</sup>. The reason of this displacement is attributed to the force imbalance under externally generated vertical field<sup>16</sup>, while the possible role played by the dynamic of relativistic electrons in a self-generated magnetic field has not been fully explored.

Similar horizontal drift of runaway orbit has been studied using test particle model<sup>19</sup>. It is found that the balancing of canonical angular momentum budget will induce a trajectory drift to compensate any change in mechanical angular momentum, resulting in horizontal motion if runaways are accelerated or decelerated. This horizontal drift is directional, as opposed to the diffusion-like behavior of stochastic scattering<sup>22,23</sup>. However, the result of Ref. 19 can not be directly applied to the aforementioned inward drift, due to the fact that the current during plateau phase is carried by runaway electrons themselves. Thus its crucial for us to go beyond test particle model and consider the runaway orbit drift as an nonlinear

process, so that any drift relative to the magnetic axis will result in further displacement of axis itself.

In this paper, the aforementioned inward drift is studied by considering the current carrying runaway electrons in an 2D equilibrium during runaway plateau phase. Those runaways are being decelerated by effective radiation drag as the original inductive accelerating field is greatly reduced during plateau<sup>20</sup>. It is found that the runaway current always move inward due to the balance between canonical angular momentum change and mechanical angular momentum input if their momentum is decreasing. It is also found that the eddy current and the vertical field are important in stabilizing this inward drift. In the absence of both, the runaways will not stop until it hit the first wall even for very small amount of momentum loss. A characteristic time scale is estimated by considering the synchrotron radiation and bremsstrahlung radiation drag, and the result is found to reasonably agree with experimental observations. This agreement indicates the inward drift motion we discuss here plays an important role in understanding runaway displacement during plateau phase.

The rest of the paper will be arranged as follows. In Section II, the transit orbit of runaway electrons will be given by seeking its constant canonical angular momentum of runaways. In Section III, we consider the displacement of runaway current center for any variation of parallel momentum. The zeroth order drift of runaway current will be given as a function of runaway momentum change for both ideally conducting wall case and no wall case. Further, a characteristic time scale of such drift will be estimated using effective radiation drag. In Section IV, a conclusion of the work will be given.

## II. TRANSIT ORBIT OF RUNAWAY ELECTRONS

We consider a large aspect ratio toroidal system with major radius  $R$ , while  $R_0$  is defined as major radius corresponding to the geometry center of the poloidal cross section of the system. For simplicity, we consider the first wall to be a rectangle toroid elongated along Z direction. Let the short side of the rectangle be  $2a$ , while the long side of it be  $4a$ . The inverse aspect ratio  $\epsilon \equiv a/R_0$  is a small number. Four walls of the toroid are designated by numbers respectively.

A schematic plot of the system of interest is shown in Fig.1 along with two coordinate

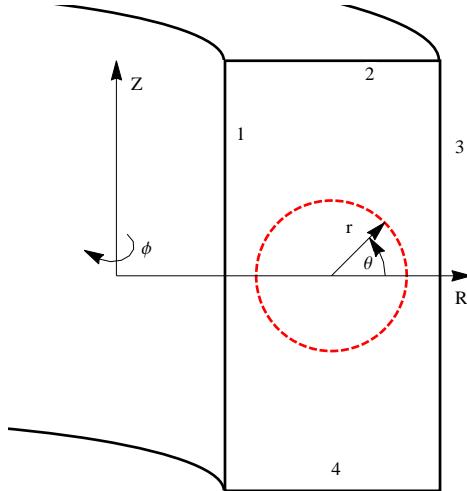


FIG. 1. A schematic plot for the cross section of the system of interest. The wall is seen as a rectangle toroid as shown in the figure by the black solid lines. The red dashed circle represent the cross section of runaway torus on this  $RZ$  plane. The two coordinate system  $(R, -\phi, Z)$  and  $(r, \theta, \phi)$  are also shown in the figure.

systems  $(R, -\phi, Z)$  and  $(r, \theta, \phi)$ . It should be noted that  $R_0$  does not necessarily correspond to the runaway current center. Since we are primarily interested in the orbit drift of runaways, no velocity space instabilities will be discussed. Also, since the vertical stability of the runaway current is essentially an equilibrium problem which is a separate topic from what we are concerned here, it will not be treated in our consideration as well.

In the absence of radiation drag, we will obtain the transit orbit of runaway electrons by seeking its constant canonical angular momentum surface. An easy way to see how this is done is to realize that the parallel momentum  $p_{\parallel}$  is a near-constant across the transit orbit for runaway electrons, as the variation of perpendicular kinetic energy  $\Delta(\mu B)$  is of  $\mathcal{O}(\epsilon^3)$  comparing to  $p_{\parallel}c$  if we assume  $p_{\perp}/p_{\parallel} \sim \epsilon$ . Thus the invariance of canonical angular momentum  $p_{\phi}(p_{\parallel}, R, -\phi, Z)$  defines a 2D trajectory surface in configuration space for runaway electrons. A more rigorous consideration would write  $p_{\parallel}$  as a function of Hamiltonian  $H$  and configuration space coordinates  $p_{\parallel}(H, R, -\phi, Z)$ , then we have  $p_{\phi} = p_{\phi}(H, R, -\phi, Z)$ . The invariance of  $H$  and  $p_{\phi}$  in time again defines the trajectory surface<sup>21</sup>. It should be noted that, due to the separation of time scale between the runaway electron's bounce time and their deceleration time, the trajectory within one bounce period can still be defined by the near-conservation of canonical angular momentum even when the radiation drag is included.

In our consideration, all of the runaways are assumed to be located on a torus with minor radius  $a_R$ , and with a single energy and pitch angle. While this is certainly not realistic, it serves to demonstrate the most fundamental physical idea. In reality, the runaway electrons have a distribution both in configuration space and in velocity space, but the well known hollowed image of runaway radiation strongly suggest a hollowed spatial profile which peaks at certain minor radius<sup>17,24,25</sup>, justifying our spatial assumption for the runaways as a zeroth order approximation. On the other hand, the single energy assumption is intended to mimic the “bump on tail” distribution of runaways in velocity space, as well as to greatly simplify the model. The effect of eddy current as a result of current center motion is taken into account by considering a simplified ideally conducting wall. This ideally conducting wall will stabilize current displacement, thus serving as a maximum stabilization scenario. In real tokamak, it’s effect will be reduced by finite resistivity.

Since assuming all the runaways are of the same energy and pitch angle, its sufficient for us to write down the Lagrangian of a single runaway electron to describe dynamic of the whole runaway torus. We write down the relativistic guiding center Lagrangian for runaways in the absence of radiation as follows<sup>19</sup>,

$$L(\mathbf{x}, \dot{\mathbf{x}}, t) = \left[ e(\mathbf{A}_R + \mathbf{A}_w + \mathbf{A}_{ex} + \mathbf{A}_c) + p_{\parallel} \hat{b} \right] \cdot \dot{\mathbf{x}} - \gamma mc^2. \quad (1)$$

Here,  $e$  is the charge of electron,  $m$  is electron mass,  $c$  is the speed of light,  $\hat{b}$  denotes the direction of magnetic field which is largely in toroidal direction due to the strong toroidal guide field.  $\gamma$  is the relativistic factor

$$\gamma = \sqrt{1 + \frac{p_{\parallel}^2}{m^2 c^2} + \frac{2\mu B}{mc^2}}. \quad (2)$$

$B$  stand for the magnetic field, and the magnetic momentum is  $\mu \equiv p_{\perp}^2/2mB$ , while  $p_{\parallel}$  and  $p_{\perp}$  are the momentum parallel and perpendicular to the field line, respectively.

We now look at the contribution from vector potentials term by term,  $\mathbf{A}_R$  is the vector potential generated by the runaway current,  $\mathbf{A}_w$  is the vector potential corresponding to eddy current generated in a ideally conducting wall as a reaction to runaway current motion. Thus  $\mathbf{A}_R + \mathbf{A}_w$  describe the total vector potential of a runaway current loop surrounded by the first wall. Apart form those contributions,  $A_{ex}$  corresponds to an additional toroidal electric field which is generated by external coil and has the following form,

$$\mathbf{E}_{ex}(R) = -\frac{\partial \mathbf{A}_{ex}}{\partial t}, \quad (3)$$

$$\mathbf{E}_{ex} = E_{ex0} \frac{R_0}{R} \hat{\phi}. \quad (4)$$

We should point out that, since we are considering runaway electrons with high energy, the current carried by those electrons is just

$$I_R = N_R e c. \quad (5)$$

Here,  $N_R$  is the total runaway population. Hence we know that the kinetic energy change of those electrons will only have minimal impact on the current itself, so that the inductive electric field from the change of poloidal magnetic flux is negligible. In a more realistic consideration, the distribution of runaways in velocity space has to be considered, and there may be small inductive field exist due to low energy runaways slowing down thus reducing the runaway current. However, those inductive field would be much smaller than the toroidal field at the beginning of current quench due to the much slower current decay rate.

Last, there is an additional contribution  $\mathbf{A}_c$  representing the constant magnetic field imposed by external coils, which include a toroidal field along  $\phi$  direction and a vertical field along  $Z$  direction

$$\mathbf{B}_c = \mathbf{B}_T + \mathbf{B}_Z, \quad (6)$$

$$\mathbf{B}_T = -\frac{B_{T0}R_0}{R} \hat{\phi}, \quad \mathbf{B}_Z = B_{Z0} \hat{z}. \quad (7)$$

The vertical field here represents the externally applied position control field, which will keep the current at the center of the system at the beginning of our consideration. It serves as a simplified mimic of the horizontal position control field in a real tokamak, as it is constant in space and time, as opposed to the real field which varies in both. Nonetheless, any gradual spatial variation or active position control can be treated as additional effects, while we are only concerned with the fundamental trend of runaway drift here. Due to the form of those constant field,  $\mathbf{A}_c$  can be chosen to have the following form

$$\mathbf{A}_c = \frac{1}{2} \ln \left( \frac{R}{R_0} \right) R_0 B_{T0} \hat{z} - \frac{R_0 B_{T0} z}{2R} \hat{R} + \frac{1}{2} B_{Z0} R \hat{\phi}. \quad (8)$$

Only the  $\phi$  component of  $\mathbf{A}_c$  will contribute to the trajectory of runaway electrons. The constant  $B_{Z0}$  is chosen so that at the beginning of the runaway plateau the runaway current center coincide with the geometry center of the system  $R_0$ .

Now the vector potential contribution from the runaway current itself will be write down explicitly. We assume *a priori* that the radial variation of runaway orbit along  $\theta$  direction is of  $\mathcal{O}(\epsilon a_R)$ , so that the poloidal cross-section of runaway orbit can be approximated as a circle. Hence the magnetic field directly generated by the runaway current is axis-symmetric with regard to the runaway current center in the large aspect ratio limit. We will check the validity of this assumption *a posteriori*. This yields the following simple contribution

$$\mathbf{B}_\theta = \frac{\mu_0 I_R}{2\pi r} \hat{\theta}, \quad (9)$$

$$\mathbf{A}_R = -\frac{\mu_0 I_R R_0}{2\pi R} \left[ \ln \left| \frac{r}{a} \right| K(r - a_R) + \ln \left| \frac{a_R}{a} \right| I(r - a_R) \right] \hat{\phi}, \quad (10)$$

$$K(x) = 1, \quad (x \geq 0); \quad K(x) = 0, \quad (x < 0); \quad I(x) = 1 - K(x). \quad (11)$$

Here,  $r$  is the minor radius of runaway electrons relative to the runaway current center. The step function  $K$  and  $I$  represent the fact that there is no current within the runaway torus, thus the runaway current contribution to the poloidal field is zero within the torus, and the vector potential have a simple  $R_0/R$  behavior. Further, the response from the ideally conducting wall will be treated by simple magnetic image method. We treat the movement  $d$  of runaway current  $I_R$  effectively as adding a pair of new current, one at the original position of the current and with value  $-I_R$  which cancels the original current, the other at distance  $d$  and with value  $I_R$  which represents the moved current. The image currents corresponding to those two effective currents then represent the eddy current contribution to current center displacement. A schematic plot of this treatment is shown in Fig. 2.

This yields

$$\mathbf{A}_w = \mathbf{A}_w^{(+)} + \mathbf{A}_w^{(-)}, \quad (12)$$

$$\mathbf{A}_w^{(+)} = \frac{\mu_0 I_R R_0}{2\pi R} \left( \ln \left| \frac{r_1^{(+)}}{a} \right| + \ln \left| \frac{r_2^{(+)}}{a} \right| + \ln \left| \frac{r_3^{(+)}}{a} \right| + \ln \left| \frac{r_4^{(+)}}{a} \right| \right) \hat{\phi}, \quad (13)$$

$$\mathbf{A}_w^{(-)} = -\frac{\mu_0 I_R R_0}{2\pi R} \left( \ln \left| \frac{r_1^{(-)}}{a} \right| + \ln \left| \frac{r_2^{(-)}}{a} \right| + \ln \left| \frac{r_3^{(-)}}{a} \right| + \ln \left| \frac{r_4^{(-)}}{a} \right| \right) \hat{\phi}. \quad (14)$$

Here,  $r_i^{(\pm)}$  represents the distance between runaway and the positive and negative image current centers generated by corresponding wall as designated in Fig.1 respectively. For

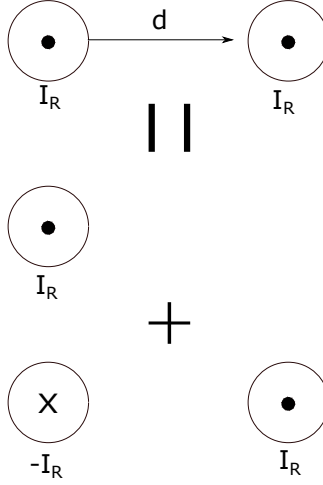


FIG. 2. A schematic plot for the treatment of current center displacement. The displaced current is effectively represented by adding two new current with value  $-I_R$  and  $I_R$  respectively.

leading order contribution, it would be well enough for us to just take the four pairs of “primary” image currents directly corresponds to the current center displacement.

Finally, using above equations, Eq. (1) can be rewritten as follows,

$$L = p_r \dot{r} + p_\theta \dot{\theta} + p_\phi \dot{\phi} - H, \quad (15)$$

$$p_r = \frac{1}{2} e \ln \left( \frac{R}{R_0} \right) R_0 B_0 \sin \theta - e \frac{R_0 B_0 z}{2R} \cos \theta, \quad (16)$$

$$p_\theta = \frac{1}{2} e \ln \left( \frac{R}{R_0} \right) R_0 B_0 r \cos \theta - e \frac{R_0 B_0 r z}{2R} \sin \theta + (p + e A_d) r \sin \alpha, \quad (17)$$

$$p_\phi = \left[ e \left( A_R + A_w + A_{ex} + \frac{1}{2} B_{z0} R \right) + p_{\parallel} \cos \alpha \right] R, \quad (18)$$

$$H = mc^2 \sqrt{1 + \frac{p_{\parallel}^2}{m^2 c^2} + \frac{2\mu B}{mc^2}}. \quad (19)$$

Here,  $\alpha$  is defined as  $\tan \alpha = B_\theta / B_T$ , so that  $\cos \alpha \sim 1$  for a large aspect ratio torus, and it can be approximately seen as a constant. It can be seen from Eq. (15) that there is no explicit dependence on  $\phi$  in the Lagrangian, so that the Euler-Lagrange equation yields

$$\frac{\partial L}{\partial \phi} = \frac{d}{dt} \left( \frac{\partial L}{\partial \dot{\phi}} \right) = \frac{d}{dt} p_\phi = 0. \quad (20)$$

That is, the symmetry of the system demands the canonical angular momentum of runaway electron to be a invariant in time. This invariant will define the surface of runaway orbit in



configuration space. In the presence of non-conservative forces such as radiation drag, the toroidal component of the modified Euler-Lagrange equation write<sup>26</sup>

$$\frac{d}{dt} \left( \frac{\partial L}{\partial \dot{\phi}} \right) - \frac{\partial L}{\partial \phi} = Q_\phi. \quad (21)$$

Here,  $Q_\phi$  corresponds to the change of angular momentum caused by radiation drag. Thus, for runaway electrons at any given time  $t$ , we have

$$p_\phi(t) = p_\phi(0) + \int_0^t Q_\phi dt. \quad (22)$$

Here,  $\int_0^t Q_\phi dt$  is the total mechanical angular momentum change caused by radiation drag. It is averaged along the trajectory of runaway electrons, thus is only the function of time.

Due to the symmetry along  $\phi$  direction, this system is essentially 2D. It would be convenience for us to express the 2D poloidal plane in terms of Cartesian coordinates for the purpose of studying runaway orbit projection in this plane. We choose  $x$  to coincide with  $R$ , and  $y$  to coincide with  $Z$ .  $x = 0$  corresponds to  $R = R_0$ , and  $y = 0$  corresponds to  $Z = 0$ . Hence the  $r$  and  $r_i^{(\pm)}$  variables in Eq. (10) and (12) can be expressed as

$$r = \sqrt{(x - d)^2 + y^2}, \quad (23)$$

$$\begin{aligned} r_1^{(+)} &= \sqrt{[x + (2a + d)]^2 + y^2}, & r_2^{(+)} &= \sqrt{(x - d)^2 + (y - 4a)^2}, \\ r_3^{(+)} &= \sqrt{[x - (2a - d)]^2 + y^2}, & r_4^{(+)} &= \sqrt{(x - d)^2 + (y + 4a)^2}, \end{aligned} \quad (24)$$

$$\begin{aligned} r_1^{(-)} &= \sqrt{(x + 2a)^2 + y^2}, & r_2^{(-)} &= \sqrt{x^2 + (y - 4a)^2}, \\ r_3^{(-)} &= \sqrt{(x - 2a)^2 + y^2}, & r_4^{(-)} &= \sqrt{x^2 + (y + 4a)^2}. \end{aligned} \quad (25)$$

Here,  $d \equiv R_c - R_0$  is the displacement of runaway current center relative to the geometric center of the system. Substituting Eq. (23) - (25) into Eq. (10) and Eq. (12), we then can seek the constant canonical angular momentum surface for runaways with a given momentum  $p_{\parallel}$  by simply solving Eq. (18). This surface defines the runaway orbit in the magnetic field considered in our model. In this section, we will consider the displaced runaway orbit for changing parallel momentum as a sequence of stationary trajectory surfaces with time dependent terms dropped, each surface corresponds to a different parallel momentum and a different displacement. Direct impression of runaway orbit drift with respect to a given change in parallel momentum can then be obtained by comparing the original runaway

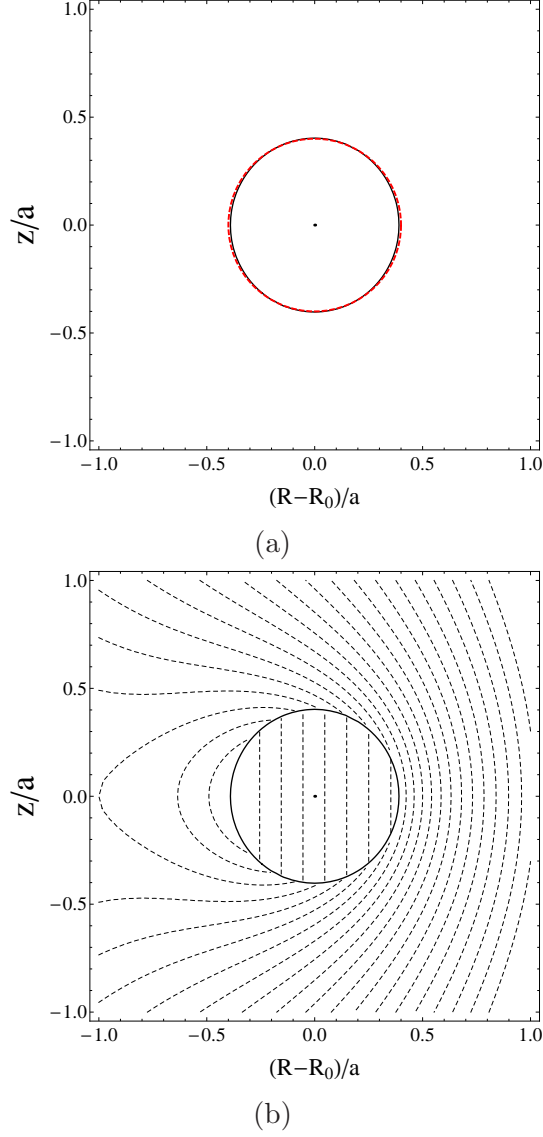


FIG. 3. The runaway electron orbit cross-section in the poloidal plane at the beginning of runaway plateau with relativistic factor  $\gamma = 100$  and  $I_R \sim 0.1$  MA. (a) The comparison between runaway orbit with current center at  $R_0$  and a circle with minor radius  $0.4a$ . The black solid line represents the runaway orbit, and the red dashed line the analytical circle. (b) The runaway orbit in the background of total vector potential contour, which is represented by black dashed lines. The black dot in both figures denotes the position of runaway current center.

orbit at the beginning of plateau with the decelerated one, as shown in Fig.3 and Fig.4 respectively. Here, the runaway current  $I_R$  acts as a given parameter and does not change in time. The radius of runaway torus is  $a_R = 0.4a$ . Further, the variation of  $p_{\parallel}$  due to the inhomogeneity of magnetic field is negligible as  $\gamma m_e c^2 \gg \mu B$ .

In Fig. 3, the runaway orbit at the beginning of runaway plateau is shown. The runaway electron parallel momentum is set to be  $p_{\parallel 0} = 2e \frac{\mu_0 I_R}{2\pi} \frac{R_0}{a}$ , the constant vertical field is chosen as  $B_{Z0} = -p_{\parallel 0}/eR_0$  so that the runaway current center will be at  $R_0$ . For runaway current on the order of  $I_R \sim 0.1$  MA, the aforementioned choice of parallel momentum corresponds to a relativistic factor  $\gamma = 100$ . The inverse aspect ratio is chosen as  $\epsilon = 0.2$ . The runaway orbit is compared with a analytical circle with minor radius being  $0.4a$  in Fig. 3 (a). In Fig. 3 (b), the orbit is put in the background of vector potential contour. The sudden change in the field behavior within the runaway torus is due to the step functions in Eq. (10), and will not affect the runaway orbit in any way. Then we consider the case when the runaways have decelerated due to radiation drag. The relativistic factor is now  $\gamma \simeq 68$ , the displacement is found by calculating the constant  $p_\phi$  contour iteratively so that the geometric center of orbit matches the current center position  $R_0 + d$ . The comparison between the orbit and a analytical circle with minor radius  $0.4a$  is also shown in Fig. 4, as well as the total vector potential contour.

The most important feature obtained from this comparison is that runaway electrons will drift inward as long as they are decelerating, which will contribute to the inward runaway current drift observed in runaway plateau regime. The detailed dynamic of this inward drift will be discussed in Section III. Also, it can be seen that the deviation of runaway transit orbit from circle is less than  $\mathcal{O}(\epsilon)$  comparing to  $a_R$ , justifying our assumption that the runaway orbit cross-section can be approximated as a circle even with substantial displacement.

### III. INWARD DRIFT OF RUNAWAY ELECTRON TRANSIT ORBIT

The runaway orbit for a given  $p_{\parallel}$  is demonstrated in Section II by iteratively seeking the constant  $p_\phi$  surface. The explicit time dependence of this orbit is dropped. However, we are also interested in the dynamic of runaway orbit drift which is more relevant to the control of current displacement. That is, we wish to know analytically how much the displacement would be for a given change in runaway momentum  $\Delta p_{\parallel}$ . The time scale of this displacement is also of interest.

This dynamic can be get by considering the energy equation for runaways along with the modified Euler-Lagrange equation. We write down the instantaneous change of both energy

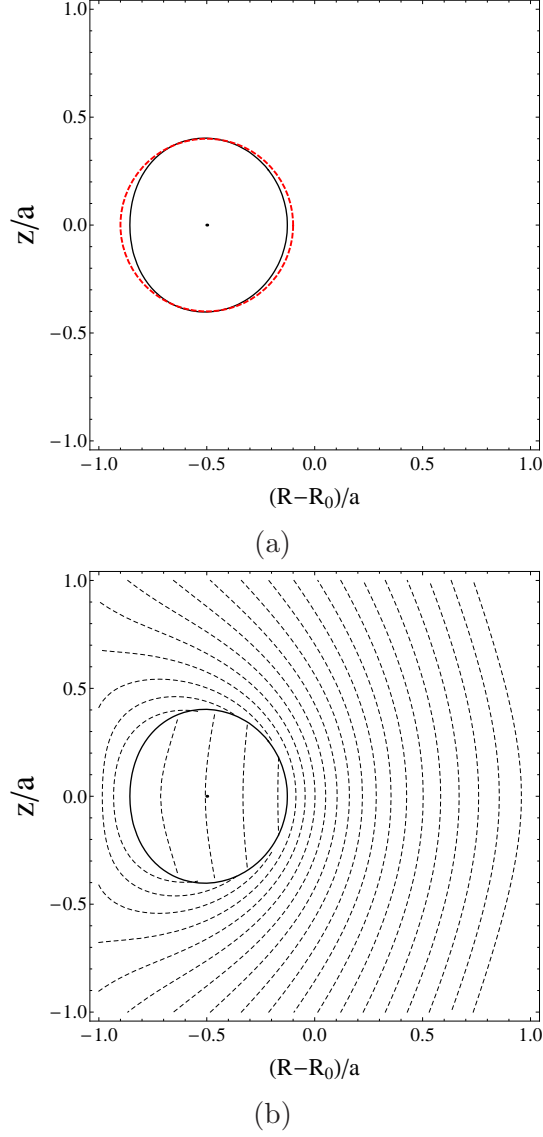


FIG. 4. The runaway electron orbit cross-section in the poloidal plane when current center displacement is  $d = -0.5a$ , corresponding  $\gamma \simeq 68$  with the same  $I_R$ . (a) The comparison between runaway orbit with current center at  $R_0$  and a circle with minor radius  $0.4a$ . The black solid line represents the runaway orbit, and the red dashed line the analytical circle. (b) The runaway orbit in the background of total vector potential contour, which is represented by black dashed lines. The black dot in both figures denotes the position of runaway current center.

and angular momentum caused by an unspecified toroidal force  $F$  as follows,

$$m_e c^2 d\gamma = F \frac{p_{\parallel}}{m_e \gamma} d\tau, \quad (26)$$

$$dp_{\phi} = FRd\tau. \quad (27)$$

Here, we have used the fact that the direction of magnetic field line is mostly toroidal. Recalling that  $p_{\parallel} = \gamma m_e c$ , we have

$$dp_{\parallel} = F d\tau. \quad (28)$$

Integrating over one bounce period  $\Delta t$ , we have

$$\Delta p_{\parallel} = \int_0^{\Delta t} F d\tau, \quad \Delta p_{\phi} = \int_0^{\Delta t} F R d\tau. \quad (29)$$

While the exact form of  $F$  is required to write down the relationship between  $\Delta p_{\parallel}$  and  $\Delta p_{\phi}$ , we will demonstrate that, for particles under effective radiation drag and externally applied toroidal electric field, we have

$$-e\Delta(A_{ex}R) + \int_0^{\Delta t} eE_d R d\tau = \Delta p_{\parallel} (R_0 + d). \quad (30)$$

Here,  $E_d$  is the effective electric field experienced by the runaway electrons.

For externally applied toroidal field,  $F$  has the following form

$$F = eE_{ex0} \frac{R_0}{R}. \quad (31)$$

Integrating along unperturbed transit orbit over one bounce period while assuming the parallel momentum and field line pitch angle being near constant within one orbit revolution, the change in momentum caused by external field is then

$$\Delta p_{\parallel}^{(ex)} = eE_{ex0} \frac{R_0}{R_0 + d} \Delta t + \mathcal{O}(\epsilon^2). \quad (32)$$

At the same time, according to Eq. (3), the change in  $A_{ex}R$  is

$$\Delta(A_{ex}R) = -E_{ex0} R_0 \Delta t. \quad (33)$$

Thus we have

$$-e\Delta(A_{ex}R) = \Delta p_{\parallel}^{(ex)} (R_0 + d). \quad (34)$$

On the other hand, we can write  $E_d = E_{sd} + E_{bd}$ , where  $E_{sd}$  and  $E_{bd}$  represent effective drag field caused by synchrotron and bremsstrahlung radiation respectively. Assuming  $\gamma$  and pitch angle being a near constant across one bounce period, we can write<sup>5,7</sup>

$$E_{sd} = E_{sd0} \frac{R_0^2}{R^2}, \quad E_{bd} = E_{bd0}. \quad (35)$$

Hence the parallel momentum change and angular momentum change can be obtained using similar integration with above to yield

$$\Delta p_{\parallel}^{(sd)} = eE_{sd0} \frac{R_0^2}{(R_0 + d)^2} \Delta t + \mathcal{O}(\epsilon^2), \quad \Delta p_{\parallel}^{(bd)} = eE_{bd0} \Delta t + \mathcal{O}(\epsilon^2), \quad (36)$$

$$\Delta p_{\phi}^{(sd)} = eE_{sd0} \frac{R_0^2}{R_0 + d} \Delta t + \mathcal{O}(\epsilon^2), \quad \Delta p_{\phi}^{(bd)} = eE_{bd0} (R_0 + d) \Delta t + \mathcal{O}(\epsilon^2). \quad (37)$$

Thus we have

$$\Delta p_{\phi}^{(d)} = \Delta p_{\phi}^{(sd)} + \Delta p_{\phi}^{(bd)} = \left( \Delta p_{\parallel}^{(sd)} + \Delta p_{\parallel}^{(bd)} \right) (R_0 + d). \quad (38)$$

Combining Eq. (34) and Eq. (38), we naturally get Eq. (30).

Armed with the knowledge of angular momentum change, we now proceed to study the drift of runaway orbit. We do this by integrating Eq. (21) over  $\Delta t$  and seek variation of  $x$  and  $d$ , namely  $\Delta x$  and  $\Delta d$ , for any given change in parallel momentum  $\Delta p_{\parallel}$ . Due to our assumption of circular cross section, we have  $\Delta x \simeq \Delta d$  and  $\Delta y \simeq 0$ . A schematic plot for  $d$ ,  $x$ ,  $\Delta d$  and  $\Delta x$  is shown in Fig. 5. Substituting Eq. (30), we write

$$e\Delta [(A_R + A_w) R] + eB_{Z0} R \Delta x + \Delta p_{\parallel} (x - d) + p_{\parallel} \Delta x = 0. \quad (39)$$

Recalling that  $B_{Z0} = -p_{\parallel 0}/eR_0$ , the above equation is then rewritten as

$$e\Delta [(A_R + A_w) R] - (p_{\parallel 0} - p_{\parallel}) \Delta x + \Delta p_{\parallel} (x - d) - p_{\parallel 0} \frac{x}{R_0} \Delta x = 0. \quad (40)$$

Eq. (40) is the most essential equation in our following analysis on the horizontal drift of runaway trajectory.

It would be convenient to discuss the two extreme case where the time scale of runaway displacement being much longer than the resistive time scale of the wall, and, conversely, the displacement time scale being much shorter than the resistive time scale. In the former case, the contribution from wall current vanish, and the constant vertical magnetic field is crucial in stabilizing the horizontal drift. In the latter case, the eddy currents from wall takes over this role, as their contribution now dominate over that of the vertical field. Here, we will first study the no wall limit, which is much simpler than the ideal wall limit. Then we will look into the more interesting ideal wall case.

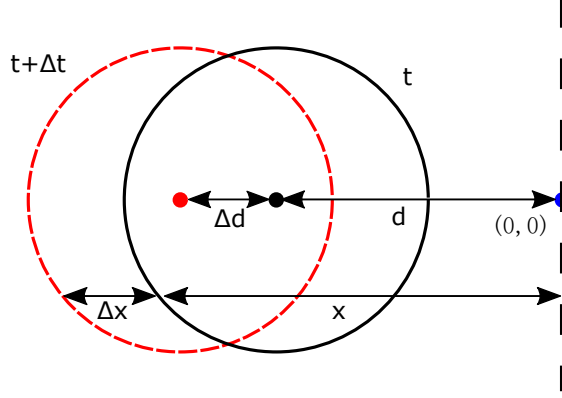


FIG. 5. A schematic plot for the runaway transit orbit at time  $t$  and  $t + \Delta t$ , with current center displacement  $d$  and  $d + \Delta d$  respectively. The relative major radial position  $x$  for a arbitrary point on the transit orbit surface, and its displacement  $\Delta x$  after  $\Delta t$  is also shown on the plot.

### A. Runaway drift dynamic with highly resistive wall

The simpler of the aforementioned two scenarios is the case where the time scale of current center drift is much longer than the resistive time scale of the wall. In this case, the wall can be seen as magnetically transparent. That is, there is no response from wall current to the change of magnetic field within the vessel.

Under this consideration,  $A_w$  vanish from Eq. (40), and we have

$$e\Delta [(A_R + A_w) R] = -e \frac{\mu_0 I_R R_0}{2\pi} \frac{y}{a_R^2} \Delta y. \quad (41)$$

It is important to recognize that the variation of  $x$  and  $d$  cancel each other in  $\Delta(A_R R)$  since  $\Delta x \simeq \Delta d$ . Also note that although assumed  $\Delta y$  being small, we still formally keep it here. We will show that it is indeed small later. For convenience, we define the following normalized parallel momentum

$$\bar{p}_{\parallel} \equiv \left( e \frac{\mu_0 I_R R_0}{2\pi} \frac{R_0}{a} \right)^{-1} p_{\parallel}. \quad (42)$$

We further expand the last term at LHS of Eq. (40) using  $x - d$ , so that Eq. (40) can be written into

$$-\frac{ay}{a_R^2} \Delta y + (\bar{p}_{\parallel} - \bar{p}_{\parallel 0}) \Delta x + \Delta \bar{p}_{\parallel} (x - d) - \bar{p}_{\parallel 0} \frac{d}{R_0} \Delta x - \frac{\bar{p}_{\parallel 0}}{R_0} (x - d) \Delta x = 0. \quad (43)$$

Since  $x$  can be chosen as any number between  $[-a_R + d, a_R + d]$ , the requirement of  $\Delta x$

having non-trivial solution for any given  $\Delta p_{\parallel}$  demands that

$$-\frac{ay}{a_R^2}\Delta y + (\bar{p}_{\parallel} - \bar{p}_{\parallel 0})\Delta x - \bar{p}_{\parallel 0}\frac{d}{R_0}\Delta x = 0, \quad (44)$$

$$\Delta x = \frac{R_0}{\bar{p}_{\parallel 0}}\Delta\bar{p}_{\parallel}. \quad (45)$$

For consistency, we must also require that

$$\frac{\partial}{\partial d}(\bar{p}_{\parallel} - \bar{p}_{\parallel 0}) = \frac{\Delta\bar{p}_{\parallel}}{\Delta d} = \frac{\Delta\bar{p}_{\parallel}}{\Delta x}. \quad (46)$$

These requirements yield the following solution of equation

$$\bar{p}_{\parallel} - \bar{p}_{\parallel 0} = \bar{p}_{\parallel 0}\frac{d}{R_0}, \quad (47)$$

$$\Delta y = 0. \quad (48)$$

It can be seen that the runaway torus drift exactly in a rigid body manner. Also, the runaway current drift and the total change in parallel momentum has a clean and simple linear relation, and the runaway electrons will drift inward as long as they are decelerating. This linear behavior derive from the fact that the prescribed vertical field is the dominant stabilizing term in the drift equation for no wall limit, rather than the wall current term which is dependent on the runaway current displacement. It can be further inferred that the runaways would hit the wall even for some small change in momentum on the order  $|p_{\parallel} - p_{\parallel 0}| \sim \mathcal{O}(\epsilon)$ .

This result is essentially along the same line with the scenario studied by Guan et al. in Ref. 19, as both cases concerns the drift of runaway electrons in a prescribed magnetic field. The only difference is that Guan et al. studied the outward drift of accelerating runaways in a constant poloidal field carried by plasma current, while here we are looking at the inward drift of decelerating runaways in a constant vertical field sustained by external coils.

It is desirable for us to estimate the time scale of aforementioned horizontal drift caused by effective radiation drag. This can be done by combining Eq.(36) and Eq.(45), and estimating the no wall limit drift time scale as  $\tau_{nw} = a/(\Delta x/\Delta t)$ . For our case considered here,  $I_R = 0.1\text{MA}$ ,  $\epsilon = 0.2$ , so that  $\frac{\mu_0 I_R R_0}{2\pi a} = 1 \times 10^{-1}\text{V} \cdot \text{s}/\text{m}$ , The effective drag field can be estimated by considering synchrotron radiation and bremsstrahlung radiation<sup>5,7</sup>, with  $\gamma_0 \sim 100$ ,  $B_{T0} \sim 3\text{T}$ , and  $R_0 = 5\text{m}$ . The resulting effective drag field is on the order of 1.19 V/m. Hence the characteristic time scale of runaway orbit drift is  $\tau_d \sim 3.4 \times 10^{-2}\text{s}$ .



## B. Runaway drift dynamic with ideally conducting wall

Now, we proceed to consider the case where the time scale of runaway displacement is much shorter than the resistive time of the wall. Thus the wall can be seen as ideally conducting as studied in Section II. The algebra is more complicated than that of Section III A due to the complicated nature of  $A_w$ , but the method is along the same line.

To simplify the expression, we now formally write  $\Delta [(A_R + A_w) R]$  in term of  $\Lambda^{(i)}(x, d, y) \Delta x + M^{(i)}(x, d, y) \Delta y$ , where  $\Lambda^{(i)}$  and  $M^{(i)}$  have the dimension of inverse length. So that

$$e\Delta (A_R R) = -e \frac{\mu_0 I_R R_0}{2\pi} [\Lambda \Delta x + M \Delta y], \quad (49)$$

$$e\Delta (A_w^{(+)} R) = e \frac{\mu_0 I_R R_0}{2\pi} [\Lambda^{(+)} \Delta x + M^{(+)} \Delta y], \quad (50)$$

$$e\Delta (A_w^{(-)} R) = -e \frac{\mu_0 I_R R_0}{2\pi} [\Lambda^{(-)} \Delta x + M^{(-)} \Delta y]. \quad (51)$$

The detailed expression for each term is then as follows.

Once again, the contribution from runaway current itself is

$$e\Delta (A_R R) = -e \frac{\mu_0 I_R R_0}{2\pi} \frac{\Delta r}{a_R} = -e \frac{\mu_0 I_R R_0}{2\pi} \frac{y}{a_R^2} \Delta y. \quad (52)$$

Meanwhile, the contribution from eddy current is

$$e\Delta (A_w^{(\pm)} R) = \pm e \frac{\mu_0 I_R R_0}{2\pi} \left[ \frac{\Delta r_1^{(\pm)}}{r_1^{(\pm)}} + \frac{\Delta r_2^{(\pm)}}{r_2^{(\pm)}} + \frac{\Delta r_3^{(\pm)}}{r_3^{(\pm)}} + \frac{\Delta r_4^{(\pm)}}{r_4^{(\pm)}} \right]. \quad (53)$$

Here, for  $A_w^{(-)}$ , we have

$$\frac{\Delta r_1^{(-)}}{r_1^{(-)}} = \frac{(x+2a)}{(x+2a)^2 + y^2} \Delta x + \frac{y}{(x+2a)^2 + y^2} \Delta y, \quad (54)$$

$$\frac{\Delta r_2^{(-)}}{r_2^{(-)}} = \frac{x}{x^2 + (y-4a)^2} \Delta x + \frac{(y-4a)}{x^2 + (y-4a)^2} \Delta y, \quad (55)$$

$$\frac{\Delta r_3^{(-)}}{r_3^{(-)}} = \frac{(x-2a)}{(x-2a)^2 + y^2} \Delta x + \frac{y}{(x-2a)^2 + y^2} \Delta y, \quad (56)$$

$$\frac{\Delta r_4^{(-)}}{r_4^{(-)}} = \frac{x}{x^2 + (y+4a)^2} \Delta x + \frac{(y+4a)}{x^2 + (y+4a)^2} \Delta y. \quad (57)$$

On the other hand, for  $A_w^{(+)}$ , we have

$$\frac{\Delta r_1^{(+)}}{r_1^{(+)}} = \frac{2[x-d+2(a+d)]}{[(x-d)+2(a+d)]^2+y^2} \Delta x + \frac{y}{[(x-d)+2(a+d)]^2+y^2} \Delta y, \quad (58)$$

$$\frac{\Delta r_2^{(+)}}{r_2^{(+)}} = \frac{(y-4a)}{(x-d)^2+(y-4a)^2} \Delta y, \quad (59)$$

$$\frac{\Delta r_3^{(+)}}{r_3^{(+)}} = \frac{2[x-d-2(a-d)]}{[(x-d)-2(a-d)]^2+y^2} \Delta x + \frac{y}{[(x-d)-2(a-d)]^2+y^2} \Delta y, \quad (60)$$

$$\frac{\Delta r_4^{(+)}}{r_4^{(+)}} = \frac{(y+4a)}{(x-d)^2+(y+4a)^2} \Delta y. \quad (61)$$

It is found that  $M^{(+)} - M^{(-)}$  is two order of magnitude smaller than  $M$ , and will be omitted hereafter. Hence we can finally write down the following form,

$$e\Delta[(A_R + A_w)R] = e\frac{\mu_0 I_R R_0}{2\pi} [(\Lambda^{(+)} - \Lambda^{(-)}) \Delta x - M \Delta y]. \quad (62)$$

Also, result from Section II indicate that in ideal wall limit  $p_{\parallel} - p_{\parallel 0}$  being comparable with  $p_{\parallel 0}$ , hence the last term at the LHS of Eq. (40) is now next order effect, and can be neglected.

Using the same normalization Eq. (42), Eq. (40) in ideal wall limit can then be written as

$$a(\Lambda^{(+)} - \Lambda^{(-)}) \Delta x - aM \Delta y - (\bar{p}_{\parallel 0} - \bar{p}_{\parallel}) \Delta x + \Delta \bar{p}_{\parallel} (x-d) = 0. \quad (63)$$

Expanding  $\Lambda^{(\pm)}$  using  $x-d$ , we have

$$\Lambda^{(+)}(x, d) = \Lambda^{(+)}|_{x=d} + (\partial_x \Lambda^{(+)})|_{x=d} (x-d) + \mathcal{O}((x-d)^2), \quad (64)$$

$$\Lambda^{(-)}(x, d) = \Lambda^{(-)}|_{x=d} + (\partial_x \Lambda^{(-)})|_{x=d} (x-d) + \mathcal{O}((x-d)^2). \quad (65)$$

Once again, the requirement of non-trivial solution demands that

$$a(\Lambda^{(+)}|_{x=d} - \Lambda^{(-)}|_{x=d}) \Delta x - aM|_{x=d} \Delta y - (\bar{p}_{\parallel 0} - \bar{p}_{\parallel}) \Delta x = 0, \quad (66)$$

$$\Delta x = -\frac{x-d}{a} [(\Lambda^{(+)} - \Lambda^{(+)}|_{x=d}) - (\Lambda^{(-)} - \Lambda^{(-)}|_{x=d})]^{-1} \Delta \bar{p}_{\parallel}. \quad (67)$$

Also, for consistency, we require that,

$$\frac{\partial}{\partial d} (\bar{p}_{\parallel} - \bar{p}_{\parallel 0}) = \frac{\Delta \bar{p}_{\parallel}}{\Delta d} = \frac{\Delta \bar{p}_{\parallel}}{\Delta x}. \quad (68)$$

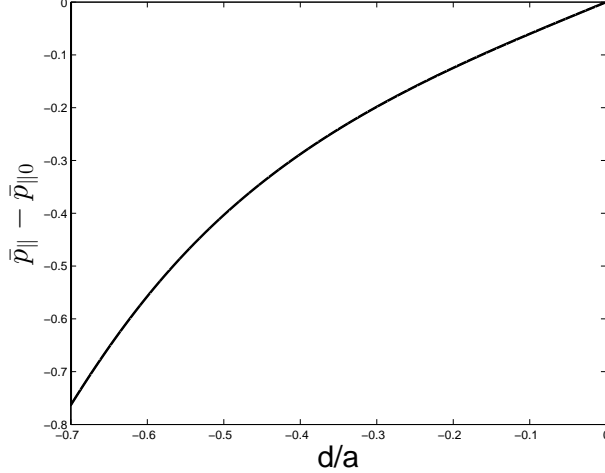


FIG. 6. The relation between runaway current center displacement  $d$  and the total change in normalized parallel momentum  $\bar{p}_{\parallel} - \bar{p}_{\parallel 0}$ . It is assumed that  $a = 1$  and  $a_R = 0.3$ .

Taking the limit  $x \rightarrow d$ , Eq. (67) then can be solved numerically by simple 4th order Runge-Kutta method<sup>27</sup> to obtain the displacement of runaway torus regarding to any parallel momentum change. The result of numerical integration is shown in Fig. 6 for parameters  $a = 1$  and  $a_R = 0.3$ . Again, it can be seen that the runaway electrons will drift inward as long as they are losing momentum, regardless of the detailed history of deceleration.

It is noteworthy that the orbit displacement described by Eq. (67) is not that of a rigid body, as opposed to the no wall limit case. Indeed, it can be seen from Eq. (66) and Eq. (67) that  $\Delta x$  is actually dependent on  $x - d$ , and  $\Delta y$  is not exactly zero. This corresponds to the “squeeze” of runaway torus cross-section seen in Fig. 4. Thus it is desirable for us to check the magnitude of  $\Delta y$  and  $\Delta x - \Delta d$  for the consistency of our model. For this purpose, it’s possible to write down analytical solutions for  $\Delta y$ . Checking through Eq. (54) - (61), it can be shown that

$$\partial_d (\Lambda^{(+)}|_{x=d}) = 2 (\partial_x \Lambda^{(+)}|_{x=d}), \quad (69)$$

$$\partial_d (\Lambda^{(-)}|_{x=d}) = (\partial_x \Lambda^{(-)}|_{x=d}). \quad (70)$$

Hence we can infer from Eq. (66) - (68) that  $\bar{p}_{\parallel}$  has the following relation with the displacement,

$$\bar{p}_{\parallel} - \bar{p}_{\parallel 0} = \left( \Lambda^{(-)}|_{x=d} - \frac{1}{2} \Lambda^{(+)}|_{x=d} \right) a. \quad (71)$$

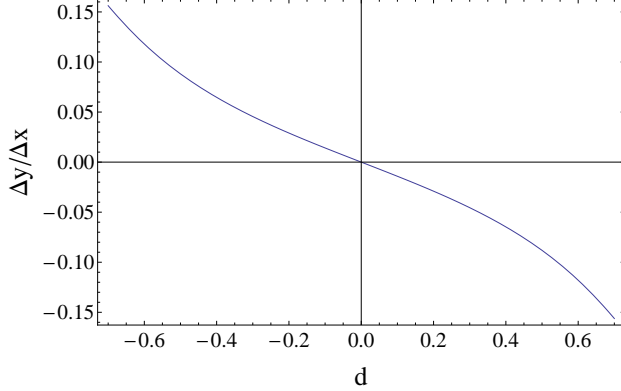


FIG. 7. The ratio between  $\Delta y$  and  $\Delta x$  as a function of displacement  $d$ , calculated assuming  $a = 1$  and  $a_R = 0.3$ . It can be seen that  $\Delta y$  is indeed much smaller than  $\Delta x$  even for substantial displacement of runaway torus, confirming the validity of our previous assumption that  $\Delta y \simeq 0$ .

Meanwhile, we also have

$$\Delta y = \frac{1}{2} (M|_{x=d})^{-1} (\Lambda^{(+)})|_{x=d} \Delta x. \quad (72)$$

The ratio  $\Delta y/\Delta x$  can then be calculated using Eq. (72) for given  $a$  and  $a_R$ . Consider  $a = 1$ ,  $a_R = 0.3$  and  $y$  being positive as an example,  $\Delta y$  turns out to be indeed much smaller than  $\Delta x$  even for substantial displacement, as can be seen in Fig. 7. Hence the vertical displacement can indeed be neglected as a next order effect, and our assumption that  $\Delta y \simeq 0$  stands valid.

Meanwhile, the deviation of  $\Delta x$  from  $\Delta d$  can be obtained by considering Eq. (67) for given  $a$ ,  $a_R$  and  $d$ . As an example, we choose  $a = 1$ ,  $a_R = 0.3$  and  $d = -0.2$ , the corresponding drift rate  $\Delta x/\Delta \bar{p}$  as a function of coordinate  $x$  is shown in Fig. 8. It can be seen that the trajectory evolution can be separated into a dominant rigid body displacement and a secondary deformation which tend to “squeeze” the runaway torus as it drift towards the wall. To demonstrate the consistency of our model, we numerically integrate Eq. (67) to show that such deformation actually have minimal impact on the over all shape of runaway cross-section until the runaways come really close to the wall. Assuming the same initial runaway torus radius and a initial normalized parallel momentum  $\bar{p}_{||0} = 2$  (which corresponds to  $\gamma \sim 100$  in our case), the displacement of both the left and right extreme points of the runaway torus, as well as that of the current center is shown in Fig. 9. It is apparent that the deformation of torus cross-section only becomes important when the current center is rather close to the wall,

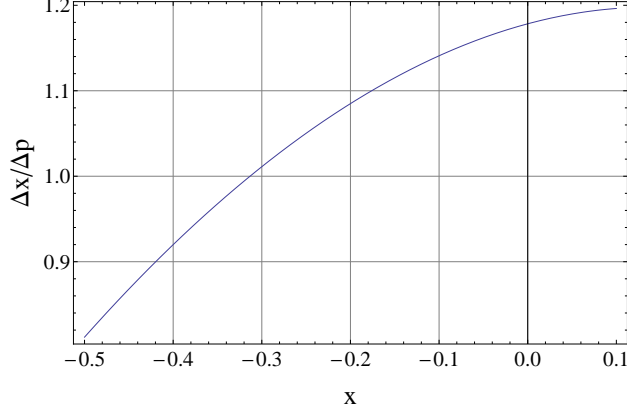


FIG. 8. The drift rate  $\Delta x/\Delta\bar{p}_{\parallel}$  as a function of  $x$  for  $a = 1$ ,  $a_R = 0.3$  and  $d = -0.2$ . At  $x = d$ , we have  $\Delta x = \Delta d$ . It can be seen that the trajectory displacement can be divided into a dominant rigid body displacement and a secondary deformation.

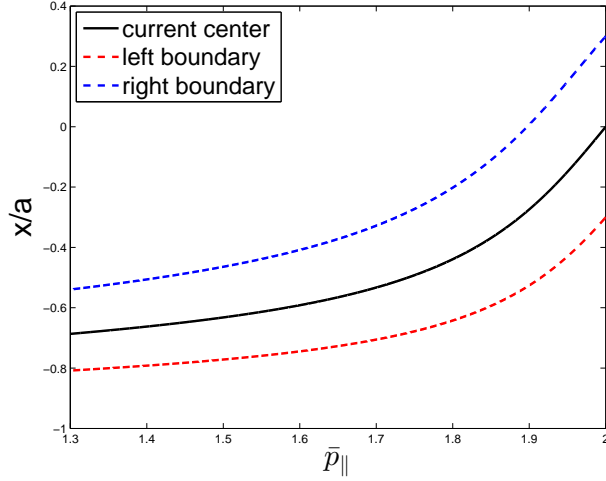


FIG. 9. The position of current center and both extreme points of the runaway torus as functions of the current center displacement. It can be seen that there is only minimal deformation of the circular even for significant displacement of current center.

We can also estimate the time scale of horizontal drift in ideal wall limit by considering the deceleration caused by radiation drag. Once again, we have,  $\frac{\mu_0 I_R R_0}{2\pi a} = 1 \times 10^{-1} V \cdot s/m$ , and the effective radiation drag can still be estimated as on the order of 1.19 V/m. At the same time, when the runaway torus is not so close to the war, the drift rate  $\Delta x/\Delta\bar{p}_{\parallel} \sim \mathcal{O}(1)$ , hence the characteristic time scale of horizontal drift is  $\tau_d \sim 8.4 \times 10^{-2} s$ . This time scale reasonably agree with experimental observation, where the current center moves one third of the minor radius in 25ms<sup>17</sup>. This corresponds to a time scale about  $8.75 \times 10^{-2} s$ . It should be noted that the estimation here is made by using the radiative drag experienced

by  $\gamma \sim 100$  runaways, as the runaway decelerate, the drift velocity is expected to be slower, hence the actual time for runaways to hit the wall may be somewhat longer than estimated here.

#### IV. DISCUSSION AND CONCLUSION

The inward drift of runaway current center during runaway plateau is studied in this paper. This horizontal drift motion is required by the balance between change in canonical angular momentum and the mechanical angular momentum change caused by radiation drag. We are mainly interested in the plateau regime after disruption where most of the current is carried by runaway electrons themselves. In this consideration, for any drift of runaway electron relative to the field line, the current center itself will also drift. Since the magnetic field lines is generated by this runaway current, the resulting current center drift motion is essentially non-linear, as opposed to the linear drift motion of test particle runaways studied in previous works<sup>19</sup>.

The runaway transit orbit surface is obtained by seeking the constant canonical angular momentum surface in a unperturbed 2D equilibrium. It is found that runaways will always drift inward as long as they are losing momentum. The eddy current and external vertical field are found to play a crucial role in stabilizing this horizontal drift, without which the runaways will not stop until they hit the first wall even for small amount of momentum loss. The dynamic of this inward drift is analyzed by taking the variation of canonical angular momentum and electron energy, which yield a first order ODE describing the trajectory displacement for any given change in parallel momentum. The remarkable feature of this drift motion is that it does not really depends on the detailed history of deceleration, only on how much momentum is lost in total. The time scale of such displacement is estimated by using models of effective radiation drag. The time scale thus calculated reasonably agrees with experimental observation.

It is noteworthy that the horizontal drift we discussed here has drastically different physics with the force imbalance along major radius, which has been invoked when discussing the observed inward motion during plateau regime<sup>16</sup>. The fundamental physics here is the balance in canonical angular momentum budget, which can not be recovered by simply

considering the runaway current as an ordinary current carrying circuit. An easy way to see this is by considering a runaway torus in perfect force balance. We then consider a certain loss of parallel momentum, with minimal decrease in the velocity of runaways. The change in  $\mathbf{J}_\phi \times \mathbf{B}_Z$  force balance is negligible, so that if we only consider the runaway current as an ordinary circuit with finite mass, the previously force balanced current will still be in equilibrium along major radial direction, thus it should not move at all. However, as we have seen in Lagrangian mechanics analysis, the runaways will actually drift inward in response to the change in mechanical angular momentum. Hence our study here provided a new powerful mechanism which may play an important role in analyzing runaway motions during plateau regime.

Strong simplification has been made to ensure the runaway current drift we concerned here to be analytically tractable. In a more realistic consideration, various more complicated model such as finite distribution of runaways in phase space and the impact of finite resistive wall should be included. Most importantly, the runaway beam with finite spatial distribution along minor radius could be of great interest, as the interaction between different “rings” of runaway torus may produce more complicated picture than that is studied here. Nonetheless, our simplified model has captured the most basic and fundamental trend for runaway trajectory behavior, namely the inward drift trend for decelerating runaways. Tracking the evolution of aforementioned more complicated model require numerical tools, and it is left for future works.

### Acknowledgments

The authors thank C. Liu, X.-G. Wang and A. Bhattacharjee for fruitful discussion. The authors also thank an anonymous referee for constructive comments. This work is partially supported by National Magnetic Confinement Fusion Energy Research Project under Grant No. 2015GB111003, National Natural Science Foundation of China under Grant No. 1126114032, 11575185, 11575186 and 11305171, JSPS-NRF-NSFC A3 Foresight Program under Grant No. 11261140328, the China Scholarship Council and US DoE contract No. AC02-09-CH11466.

## REFERENCES

- <sup>1</sup>M. N. Rosenbluth and S. V. Putvinski, Nucl. Fusion **37** 1355 (1997);
- <sup>2</sup>H. Smith, P. Helander, L.-G. Eriksson and T. Fülöp, Phys. Plasmas **12** 122505 (2005);
- <sup>3</sup>H. Smith, P. Helander, L.-G. Eriksson, D. Anderson, M. Lisak and F. Andersson, Phys. Plasmas **13** 102502 (2006);
- <sup>4</sup>T.C. Hender, J.C Wesley, J. Bialek, A. Bondeson, A.H. Boozer, R.J. Buttery, A. Garofalo, T.P Goodman, R.S. Granetz, Y. Gribov, O. Gruber, M. Gryaznevich, G. Giruzzi, S. Günter, N. Hayashi, P. Helander, C.C. Hegna, D.F. Howell, D.A. Humphreys, G.T.A. Huysmans, A.W. Hyatt, A. Isayama, S.C. Jardin, Y. Kawano, A. Kellman, C. Kessel, H.R. Koslowski, R.J. La Haye, E. Lazzaro, Y.Q. Liu, V. Lukash, J. Manickam, S. Medvedev, V. Mertens, S.V. Mirnov, Y. Nakamura, G. Navratil, M. Okabayashi, T. Ozeki, R. Paccagnella, G. Pautasso, F. Porcelli, V.D. Pustovitov, V. Riccardo, M. Sato, O. Sauter, M.J. Schaffer, M. Shimada, P. Sonato, E.J. Strait, M. Sugihara, M. Takechi, A.D. Turnbull, E. Westerhof, D.G. Whyte, R. Yoshino, H. Zohm and the ITPA MHD, Disruption and Magnetic Control Topical Group, Nucl. Fusion **47** S128 (2007);
- <sup>5</sup>J. R. Martín-Solís, J. D. Alvarez, R.Sánchez and B. Esposito, Phys. Plasmas **5** 2370 (1998);
- <sup>6</sup>F. Andersson, P. Helander and L.-G. Eriksson, Phys. Plasmas **8** 5221 (2001);
- <sup>7</sup>M. Bakhtiari, G. J. Kramer and D. G. Whyte, Phys. Plasmas **12** 102503 (2005);
- <sup>8</sup>E.M. Hollmann, M.E. Austin, J.A. Boedo, N.H. Brooks, N. Commaux, N.W. Eidietis, D.A. Humphreys, V.A. Izzo, A.N. James, T.C. Jernigan, A. Loarte, J. Martin-Solis, R.A. Moyer, J.M. Muñoz-Burgos, P.B. Parks, D.L. Rudakov, E.J. Strait, C. Tsui, M.A. Van Zeeland, J.C. Wesley and J.H. Yu, Nucl. Fusion **53** 083004 (2013);
- <sup>9</sup>P. Aleynikov and B. N. Breizman, Phys. Rev. Lett. **114** 155001 (2005);
- <sup>10</sup>J. Decker, E. Hirvijoki, O. Embreus, Y. Peysson, A. Stahl, I. Pusztai, T. Fülöp, arXiv:1503.03881v2 [physics.plasm-ph] (2015);
- <sup>11</sup>E. Hirvijoki, I. Pusztai, J. Decker, O. Embréus, A. Stahl, T. Fülöp, arXiv:1502.03333v2 [physics.plasm-ph] (2015);
- <sup>12</sup>G. Fussmann, Nucl. Fusion **19** 327 (1979);
- <sup>13</sup>P. B. Parks, M. N. Rosenbluth and S. V. Putvinski, Phys. Plasmas **6** 2523 (1999);
- <sup>14</sup>C. Liu, D. P. Brennan, A. H. Boozer and A. Bhattacharjee, arXiv:1509.04402v2 [physics.plasm-ph] (2015);



- <sup>15</sup>R. D. Gill, B. Alper, M. de Baar, T. C. Hender, M. F. Johnson, V. Riccardo and contributors to the EFDA-JET Workprogramme, Nucl. Fusion **42** 1039 (2002);
- <sup>16</sup>Eidietis, N. W. and Commaux, N. and Hollmann, E. M. and Humphreys, D. A. and Jernigan, T. C. and Moyer, R. A. and Strait, E. J. and VanZeeland, M. A. and Wesley, J. C. and Yu, J. H. Phys. Plasmas **19** 056109 (2012);
- <sup>17</sup>Y. P. Zhang, Yi Liu, G. L. Yuan, M. Isobe, Z. Y. Chen, J. Cheng, X. Q. Ji, X. M. Song, J. W. Yang, and X. Y. Song, X. Li, W. Deng, Y. G. Li, Y. Xu, and T. F. Sun, and X. T. Ding, and L. W. Yan, and Q. W. Yang, and X. R. Duan, and Y. Liu, and HL-2A Team, Phys. Plasmas **19** 032510 (2012);
- <sup>18</sup>S. V. Putvinski, P. Barabaschi, N. Fujisawa, N. Putvinskaya, M. N. Rosenbluth and J. Wesley, Plasma Phys. Control. Fusion **39** B157 (1997);
- <sup>19</sup>X. Guan, H. Qin and N. J. Fisch, Phys. Plasmas **17** 092502 (2010);
- <sup>20</sup>R. D. Gill, Nucl. Fusion **33** 1613 (1993);
- <sup>21</sup>H. Qin, X. Guan and W. M. Tang, Phys. Plasmas **16** 042510 (2009);
- <sup>22</sup>A. B. Rechester and M. N. Rosenbluth, Phys. Rev. Lett. **40** 38 (1978);
- <sup>23</sup>H. E. Mynick and J. D. Strachan, Phys. Fluids **24** 695 (1981);
- <sup>24</sup>V. V. Plyusnin, V.G. Kiptily, B. Bazylev, A.E. Shevelev, E.M. Khilkevitch, J. Mlynar, M. Lehnen, G. Arnoux, A. Huber, S. Jachmich, V. Riccardo, U. Kruezi, B. Alper, R.C. Pereira, A. Fernandes, C. Reux, P.C. de Vries, T.C. Hender and JET EFDA contributors, Proceeding of IAEA FEC2012, San Diego, USA (2012);
- <sup>25</sup>R. J. Zhou, L. Q. Hu, E. Z. Li, M. Xu, G. Q. Zhong, L. Q. Xu, S. Y. Lin, J. Z. Zhang and the EAST Team, Plasma Phys. Control. Fusion **55** 055006 (2013);
- <sup>26</sup>H. Goldstein, "Classical mechanics" (Addison-Wesley, Reading, MA, 2001), 3rd ed, p. 23;
- <sup>27</sup>J. C. Butcher, "Numerical methods for ordinary differential equations". (John Wiley & Sons, New York, 2008), p. 93;